EPJ Web of Conferences **182**, 02035 (2018) https://doi.org/10.1051/epjconf/201818202035
ICNFP 2017

Studies of low-energy K^- nuclear interactions by AMADEUS

R. Del Grande[1,2,a], M. Bazzi[1], G. Belloti[3], A. M. Bragadireanu[4], D. Bosnar[5], A. D. Butt[3,6], M. Cargnelli[7], C. Curceanu[1], L. De Paolis[1,2], L. Fabbietti[8,9], C. Fiorini[3,6], F. Ghio[10,11], C. Guaraldo[1], R. S Hayano[12], M. Iliescu[1], M. Iwasaki[13], P. Levi Sandri[1], J. Marton[7], M. Miliucci[1,2], P. Moskal[14], S. Okada[13], D. Pietreanu[4], K. Piscicchia[1,15], A. Scordo[1], H. Shi[1], M. Silarski[14], D. L. Sirghi[1,4], F. Sirghi[1,4], M. Skurzok[14], A. Spallone[1], O. Vazquez Doce[8,9], E. Widmann[7], S. Wycech[16], and J. Zmeskal[7]

[1] *INFN Laboratori Nazionali di Frascati, Frascati, Rome, Italy*
[2] *Università degli Studi di Roma Tor Vergata, Rome, Italy*
[3] *Politecnico di Milano, Dip. di Elettronica, Informazione e Bioingegneria, Milano, Italy*
[4] *Horia Hulubei National Institute of Physics and Nuclear Engineering, Magurele, Romania*
[5] *University of Zagreb, Zagreb, Croatia*
[6] *INFN Sezione di Milano, Milano, Italy*
[7] *Stefan-Meyer-Institut für Subatomare Physik, Wien, Austria*
[8] *Excellence Cluster 'Origin and Structure of the Universe', Garching, Germany*
[9] *Physik Department E12, Technische Universität München, Garching, Germany*
[10] *INFN Sezione di Roma I, Rome, Italy*
[11] *Istituto Superiore di Sanità, Rome, Italy*
[12] *The University of Tokyo, Tokyo, Japan*
[13] *RIKEN, The Institute of Physics and Chemical Research, Saitama, Japan*
[14] *Institute of Physics, Jagiellonian University, Kracow, Poland*
[15] *Museo Storico della Fisica e Centro Studi e Ricerche Enrico Fermi, Rome, Italy*
[16] *National Centre for Nuclear Research, Warsaw, Poland*

Abstract. The goal of the AMADEUS experiment is to shed light on unsolved fundamental issues in the non-perturbative strangeness QCD sector through the study of low-energy K^- hadronic interactions with light nuclear targets. The main open questions are the controversial nature of the $\Lambda(1405)$ state, which is investigated in hyperon-pion correlation studies, and the possible existence of exotic antikaon multi-nucleon clusters, whose search in K^- induced reactions is intimately related to the studies of the K^- multi-nucleon absorption processes in hyperon-nucleon/nucleus channels. The DAΦNE collider at the INFN-LNF provides unique monochromatic low-momentum kaons from the ϕ meson decay almost at-rest, suitable for the AMADEUS studies. The KLOE detector is exploited as an active target, in order to obtain excellent acceptance and resolution data for K^- nuclear capture on H, ^{4}He, ^{9}Be and ^{12}C, both at-rest and in-flight.

[a] e-mail: raffaele.delgrande@lnf.infn.it

1 Introduction

The AMADEUS (Anti-kaonic Matter At DAΦNE: An Experiment with Unraveling Spectroscopy) [1] collaboration aims to provide unique quality data of low-energy K^- hadronic interactions in light nuclei (e.g. H, ^{4}He, ^{9}Be and ^{12}C) in order to afford experimental constraints on the non-perturbative QCD in the strangeness sector. AMADEUS takes advantage of the low momentum (about 127 MeV/c), almost monochromatic, charged kaons provided by the decay of ϕ mesons at-rest at the DAΦNE factory [2]. The analyses presented here refers to the data acquired by the KLOE [3] collaboration during the 2004-2005 data taking campaign.

Chiral perturbation theory is not applicable in the *uds* SU(3) flavour sector due to the existence of broad hyperon resonances below the $\bar{K}N$ threshold, rendering the perturbative approach inappropriate. The non-perturbative chiral SU(3) dynamics [4–7] and the phenomenological potential approach [8, 9] are the main theoretical tools to overcome the difficulty. In both cases the $\bar{K}$ dynamics above threshold is well described because the two models are constrained to the scattering data but the sub-threshold extrapolations are in strong disagreement [10, 11]. Chiral models predict significantly weaker $\bar{K}N$ interaction with respect to phenomenological potentials approach. The position of the $\Lambda(1405)$ (I=0) state, which is experimentally observed through the decay into $(\Sigma\pi)^0$ channels, seems to depend on both the observed decay channel and on the production mechanism. Chiral unitary models predict the emerging of two poles contributing to the $\Lambda(1405)$ line-shape, with a high mass pole (located at about 1420 MeV) strongly coupled to the $\bar{K}N$ channel [6, 7, 10, 12], whereas the phenomenological potentials models expect the existence of a single pole of the scattering amplitude at 1405 MeV [8, 9, 13].

The position of the $\Lambda(1405)$ is related to the strength of the $\bar{K}N$ potential which also determines the possible formation of more exotic K^- multi-nucleon clusters. The lightest kaonic bound state is the di-baryonic K^-pp cluster (and the isospin partner $\bar{K}^0np$), whose main decay channels are the Λp and $\Sigma^0 p$ final states. The theoretical expectations about the position of this state are controversial, delivering a wide range of binding energies and widths [16], and the experimental findings are also contradictory [17, 18]. To obtain a deeper understanding and to interpret the ambiguity between the available results, exclusive measurements from other experiments are still necessary. The authors of Refs. [19] stressed that the search of the kaonic nuclear clusters in K^- induced reactions has to be performed with a clear knowledge of the yields and kinematic shapes of the K^- multi-nucleon absorptions, since they overlap over a broad range of the phase space with the bound states.

In Section 2 the features of the DAΦNE accelerator and the KLOE detector are summarized. In Section 3 the event selection procedure is described. Sections 4 and 5 are dedicated to the obtained results, and ongoing analyses, regarding K^- multi-nucleon absorption processes, ppK^- states, resonant and non-resonant $Y\pi$ production in light nuclei.

2 The KLOE detector at DAΦNE

DAΦNE (Double Anular Φ-factory for Nice Experiments) is a double ring e^+e^- collider, designed to work at the center of mass energy of the ϕ particle; the ϕ meson decay produces charged kaons with low momentum ($\simeq$ 127 MeV/c) which is ideal to either stop them, or to explore the products of their low-energy nuclear absorptions.

The KLOE detector is centered around the interaction region of DAΦNE, it consists of a large cylindrical Drift Chamber (DC) [22] and a fine sampling lead-scintillating fibers calorimeter [23], all immersed in the axially simmetric magnetic field with intensity of 0.52 T, provided by a superconducting solenoid. The DC entrance wall composition is 750 μm of carbon fibre and 150 μm of aluminum foil. Dedicated GEANT Monte Carlo simulations of the KLOE apparatus show that out of the total

number of kaons interacting in the DC entrance wall, about 81% are absorbed in the carbon fibre component and remaining 19% in the aluminum foil. The KLOE DC is filled with a mixture of helium and isobutane (90% in volume ^{4}He and 10% in volume C_4H_{10}). The chamber is characterized by excellent position and momentum resolutions. Tracks are reconstructed with a resolution in the transverse $R-\phi$ plane $\sigma_{R\phi} \sim 200\,\mu$m and a resolution along the z-axis $\sigma_z \sim 2$ mm. The transverse momentum resolution for low momentum tracks ($(50 < p < 300)$MeV/c) is $\frac{\sigma_{p_T}}{p_T} \sim 0.4\%$. The calorimeter is composed of a cylindrical barrel and two endcaps, providing a solid angle coverage of 98%. The volume ratio (lead/fibers/glue=42:48:10) is optimized for a high light yield and a high efficiency for photons in the range (20-300) MeV/c. The photon detection efficiency is 99% for energies larger than 80 MeV and it falls to 80% at 20 MeV due to the cutoff introduced by the ADC and TDC thresholds. The position of the clusters along the fibers can be obtained with a resolution $\sigma_\parallel \sim 1.4\,\text{cm}/\sqrt{E(\text{GeV})}$. The resolution in the orthogonal direction is $\sigma_\perp \sim 1.3$ cm. The energy and time resolutions for photon clusters are given by $\frac{\sigma_E}{E_\gamma} = \frac{0.057}{\sqrt{E_\gamma(\text{GeV})}}$ and $\sigma_t = \frac{57\,\text{ps}}{\sqrt{E_\gamma(\text{GeV})}} \oplus 100$ ps.

The AMADEUS experiment is conceived to integrate the high acceptance and momentum resolution KLOE detector with the low momentum K^- beam of the DAΦNE collider in a future dedicated setup. As a step zero, the data collected by the KLOE collaboration during the 2004-2005 data taking, corresponding to about 1.74 fb^{-1} of total integrated luminosity, are analysed. The KLOE detector is used as an active target, the hadronic interaction of negative kaons with the materials of the apparatus being investigated.

3 Particle Identification

In the following the investigation of the K^- interactions with the KLOE materials, followed by the Σ^0p, Λt and $\Lambda\pi^-$ correlated productions in the final state, will be presented. The first step of the events selection is the $\Lambda(1116)$ identification, which proceeds through the reconstruction of the $\Lambda \rightarrow p + \pi^-$ (BR = 63.9 $\pm$0.5%) decay vertex. A resolution better than 1 mm for the Λ decay vertex inside the DC volume is found based on Monte Carlo simulations. The mean value for the $p\pi^-$ invariant mass ($M_{p\pi^-}$) is (1115.753 $\pm$ 0.002) MeV/c^2 and the resolution is σ=0.5 MeV/c^2. Only statistical error is given, the systematics is under evaluation. The distribution of the Λ decay vertex position in the radial coordinate (ρ_Λ), shown in Fig. 1, exhibits the topology of the K^- absorptions in KLOE. Four components are distinguishable, from inside to outside the K^- absorptions occur: in the DAΦNE beryllium sphere ($\sim$ 5 cm), the DAΦNE aluminated beryllium pipe ($\sim$ 10 cm), the KLOE DC entrance wall ($\sim$ 25 cm) and the long tail originated from K^- interactions in the gas filling the KLOE DC (25-200 cm).

The identification of charged particles is performed using both the dE/dx information from the DC wires and the measurement of the energy released in the electromagnetic calorimeter (EMC), as described in [1]. Σ^0 particles are reconstructed through the electromagnetic decay into $\Lambda\gamma$. The photon is identified using the energy released in the KLOE EMC [20, 21]. The position of the K^- absorption vertex (hadronic vertex) is defined as the vertex between the hyperon path and a correlated particle (proton, triton and negatively charged pion) track. As an example, the obtained resolution on the radial coordinate ($\rho_{\Lambda p}$) for the Λp vertex is 1.2 mm. Cuts on the absorption vertex radial position were optimised, based on MC simulations and a study of the Λ decay path, to select K^- absorptions in the various targets with minimal contamination from other components. More details on the particle identification procedure can be found in [18].

4 K^- multi-nucleon absorptions measurements

The Σ^0p correlated production was analysed in Ref. [18], selecting the K^- captures in ^{12}C nuclei. The goal of the analysis was to pin down the contribution of the K^- two-nucleon absorptions (2NA), in

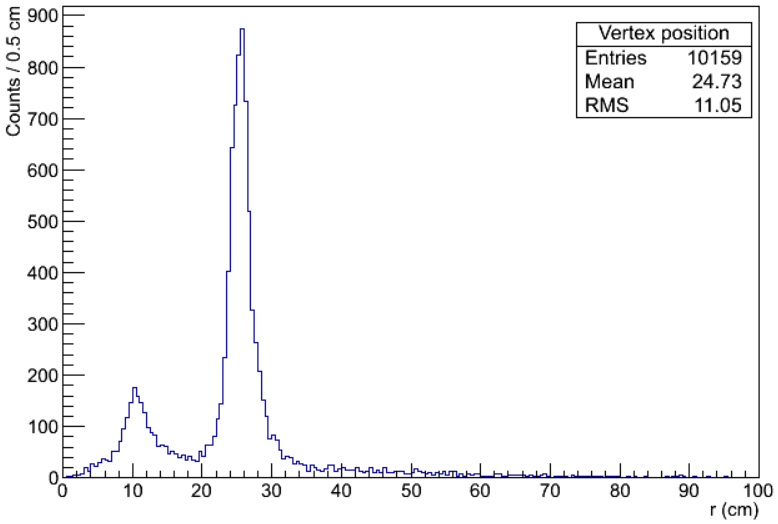

Figure 1. *Radial position distribution ρ_Λ, of the Λ decay vertex, for 2004-2005 KLOE collected data.*

order to measure the yield per stopped K^-, and to search for a possible contribution due to the K^-pp bound state formation, decaying into the $\Sigma^0 p$ channel.

A simultaneus fit of the $\Sigma^0 p$ invariant mass ($M_{\Sigma^0 p}$), the angular correlation ($\cos(\theta_{\Sigma^0 p})$), the Σ^0 and the proton momenta (P_{Σ^0} and P_p) was performed using the following contributing processes:

- $K^-A \rightarrow \Sigma^0 p_{spec}\ \pi A'$ (1NA),
- $K^-pp \rightarrow \Sigma^0 p$ (2NA),
- $K^-ppn \rightarrow \Sigma^0 pn$ (3NA),
- $K^-ppnn \rightarrow \Sigma^0 pnn$ (4NA).

The final state interactions (FSI) of the Σ^0 and p with the residual nucleus emerging from a K^-pp capture in Carbon were taken into account. The fit is shown in Fig 2.

The yield of the 2NA, when the produced Σ^0 and p particles are free form any FSI process (2NA-QF), was measured for the first time, with good precision. More difficult is to disentangle the 3NA from 2NA + FSI processes due to their similar expected shapes. The obtained results are summarized in Table 4. A second fit was performed including a K^-pp component, decaying into $\Sigma^0 p$. A systematic scan of possible binding energies and widths, varying within (15÷75) MeV and (30÷70) MeV/c^2 respectively, was performed. The best fit resulted in a binding energy of 45 MeV and a width of 30 MeV/c^2. The resulting yield normalised to the number of stopped K^- is $K^-pp/K^-_{stop} = (0.044 \pm 0.009 stat^{+0.004}_{-0.005} syst) \times 10^{-2}$. The significance of the bound state with respect to a statistical fluctuation was checked by means of an F-test. The significance of the K^-pp contribution was found to be 1σ, which is not enough to claim the measurement of a bound state signal [18].

The study of the Λt correlated production following the K^- capture in the DC gas is presently ongoing. The goal of this analysis is to measure the, extremely rare, 4NA absorption process of the K^-, selecting the captures of the negatively charged kaons on Helium ($K^- + {}^4He \rightarrow \Lambda t$). Some Λt events were identified in [24, 25] but the 4NA contribution was not extracted. In our work the

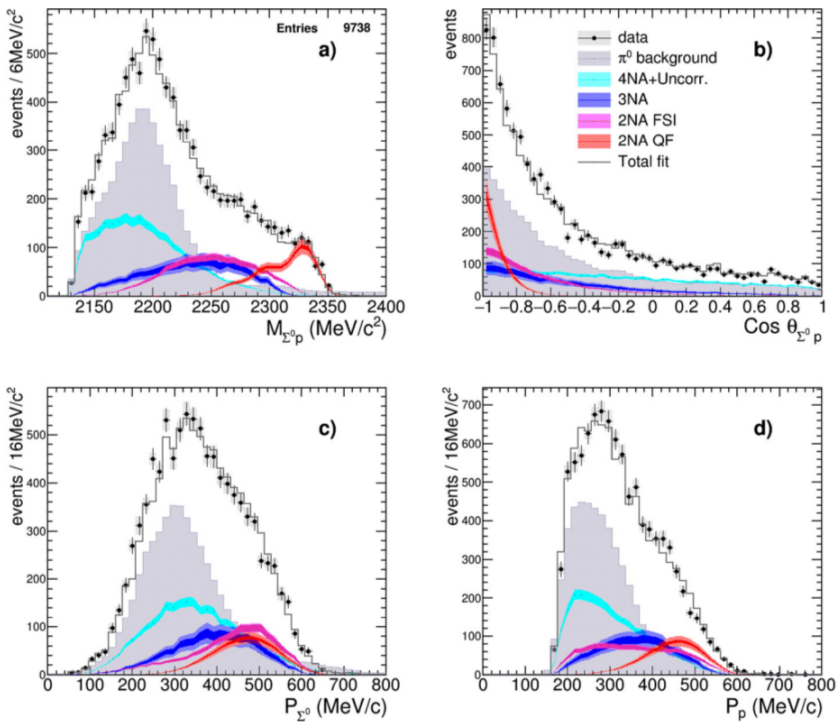

Figure 2. *Fit of the $\Sigma^0 p$ invariant mass, $cos(\theta_{\Sigma^0 p})$, Σ^0 and proton momenta is shown. Data points are represented by black circles, the systematic errors by boxes, coloured distributions correspond to the simulated processes (light-coloured bands show the statistical errors and the darker bands represent the symmetrised systematic errors). The gray line is the total fit.*

Process	yield / $K^-_{stop} \times 10^{-2}$	$\sigma_{stat} \times 10^{-2}$	$\sigma_{syst} \times 10^{-2}$
2NA-QF	0.127	±0.019	$^{+0.004}_{-0.008}$
2NA-FSI	0.272	±0.028	$^{+0.022}_{-0.023}$
Tot 2NA	0.399	±0.033	$^{+0.023}_{-0.032}$
3NA	0.274	±0.069	$^{+0.044}_{-0.021}$
Tot 3 body	0.546	±0.074	$^{+0.048}_{-0.033}$
4NA + bkg.	0.773	±0.053	$^{+0.025}_{-0.076}$

Table 1. Production probability of the Σ^0p final state for different intermediate processes normalised to the number of stopped K^- in the DC wall. The statistical and systematic errors are shown as well [18].

highest statistics ever of correlated Λt production was evidenced (150 events). The preliminary Λt invariant mass and angular correlation distributions are shown in Fig. 3 left and right respectively. The signature of K^- 4NA in ^{4}He is the production of back-to-back Λt pairs, with the highest energy permitted by the kinematics. Such events are represented in red in Fig. 3, and correspond to the cut $cos\theta_{\Lambda t} < -0.95$. This analysis is presently under finalization.

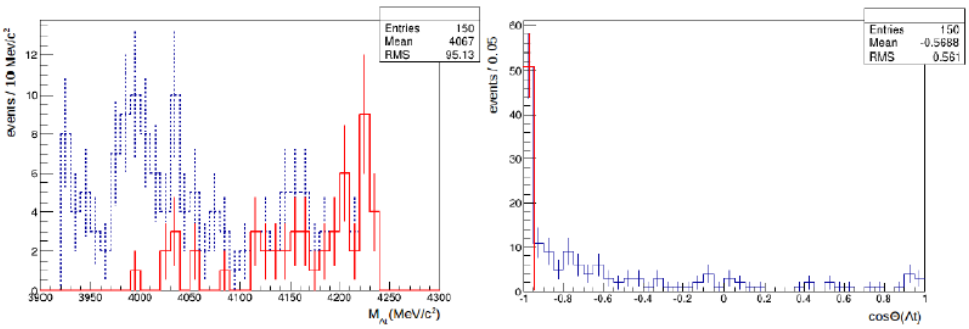

Figure 3. *(Colour online.)* Λt *invariant mass (left) and* $cos\theta_{\Lambda t}$ *(right). The events corresponding to the* $cos\theta_{\Lambda t} < -0.95$ *selection are shown in red.*

5 $\Lambda\pi^-$ resonant and non resonant production

The possibility to produce $\bar{K}$ multi-N bound states is strongly related to the strength of the $\bar{K}N$ attractive interaction, which also determines the position of the $\Lambda(1405)$ state. In K^- induced reactions, the $(\Sigma\pi)^0$ invariant mass resonant shape is influenced by the kinematic energy limit, imposed by the last nucleon binding energy. This limit is at about 1412 MeV/c^2 and 1416 MeV/^{2}, for K^- capture at-rest in ^{4}He and ^{12}C respectively. A second bias is represented by the non-resonant $\Sigma\pi$ formation, which gives rise to highly correlated hyperon-pion pairs, with narrow (of the order of 10 MeV) $M_{\Sigma\pi}$ invariant masses spectra peaked just below the kinematic limit, as shown in Ref. [26]. The $\Lambda\pi$ and $\Sigma\pi$ non resonant production, for K^- capture in light nuclear targets was never measured.

The study of the $\Lambda\pi^-$ correlated production for K^- captures in ^{4}He is presently ongoing. The goal is to measure the I=1 contribution of the non-resonant $Y\pi$ production ($K^-n \rightarrow \Lambda\pi^-$), for the first time. The advantage to investigate the I=1 channel is represented by the precise knowledge of the $\Sigma^-(1385)$ resonant transition amplitude. The Λ and π^- kinematic distributions for K^- captures in ^{4}He, both at-rest and in-flight, were calculated in Ref. [27]. The momentum probability distribution functions, of the emerging hyperon pion-pairs, following K^-n absorptions, are expressed in terms of the K^-n transition amplitudes: the isospin $I = 1$ S-wave non- resonant amplitude ($|f^{nr}|$) and the resonant $I = 1$ P-wave amplitude, dominated by the $\Sigma^-(1385)$. Since the resonant amplitude is well known, the measured total momentum distributions can be used to extract the non-resonant $|f^{nr}|$ amplitude module below the $\bar{K}N$ threshold.

Such measurement will also help to characterize the corresponding $(\Sigma\pi)^0$ $I = 0$ non-resonant transition amplitude, with the aim to extract the $\Lambda(1405)$ resonant shape.

Acknowledgement

We acknowledge the KLOE Collaboration for their support and for having provided us the data and the tools to perform the analysis presented in this paper. We acknowledge the CENTRO FERMI - Museo Storico della Fisica e Centro Studi e Ricerche “Enrico Fermi”, for the project PAMQ. Part of this work was supported by the Austrian Science Fund (FWF): [P24756-N20]; Austrian Federal Ministry of Science and Research BMBWK 650962/0001 VI/2/2009; the Grantïn-Aid for Specially Promoted Research (20002003), MEXT, Japan; the Croatian Science Foundation, under project 1680; Minstero degli Affari Esteri e della Cooperazione Internazionale, Direzione Generale per la Promozione del Sistema Paese (MAECI), Strange Matter project; Polish National Science Center through grant No. UMO-2016/21/D/ST2/01155.

References

[1] C. Curceanu, K. Piscicchia et al., Acta Phys. Polon. B46 1, 203-215, (2015).
[2] R. Baldini et al., Proposal for a Phi-Factory, report LNF-90/031(R) (1990).
[3] F. Bossi, E. De Lucia, J. Lee-Franzini, S. Miscetti, M. Palutan and KLOE coll., Riv. Nuovo Cim. 31 (2008) 531-623
[4] N. Kaiser, P. Siegel, and W. Weise, Nucl. Phys. A594, 325 (1995).
[5] E. Oset and A. Ramos, Nucl. Phys. A635, 99 (1998).
[6] J. Oller and U. G. Meißner, Phys. Lett. B500, 263 (2001).
[7] T. Hyodo and D. Jido, Prog. Part. Nucl. Phys. 67, 55 (2012).
[8] Y. Akaishi, T. Yamazaki, Phys. Rev. C65, 044005 (2002).
[9] N. V. Shevchenko, Phys. Rev. C85, 034001 (2012).
[10] T. Hyodo and W. Weise, Phys. Rev. C77, 035204 (2008).
[11] S. Ohnishi, Y. Ikeda, T. Hyodo, and W. Weise, Phys. Rev. C 93, 025207 (2016).
[12] D. Jido, J. Oller, E. Oset, A. Ramos, and U. Meißner, Nucl. Phys. A725, 181 (2003).
[13] J. Esmaili et al., Phys. Lett. B 686 (2010) 23-28
[14] C. Patrignani et al. (Particle Data Group), Chin. Phys. C, 40, 100001 (2016).
[15] T. Hyodo, D. Jido, Prog. Part. Nucl. Phys. 67 (2012) 55.
[16] T. Yamazaki, *et al.*, Phys. Rev. C **76** 045201 (2007)
A. Doté, *et al.*, Phys. Rev. C **79** 014003 (2009)
S. Wycech, *et al.*, Phys. Rev. C **79** 014001 (2009)
N. Barnea, *et al.*, Phys. Lett. B **712** 132 (2012)
N.V. Shevchenko, *et al.*, Phys. Rev. Lett. **98** 082301 (2007)
Y. Ikeda, *et al.*, Phys. Rev. C **79** 035201 (2009)
E. Oset, *et al.*, Nucl. Phys. A **881** 127 (2012)
P. Bicudo, Phys. Rev. D **76** 031502(R) (2007)
J. Revai *et al.*, Phys. Rev. C **90** 034004 (2014)
S. Maeda *et al.*, Proc. Jpn. Acad. B **89** 418 (2013)
M. Bayar and E. Oset, Nucl. Phys. A **914** 349 (2013).
[17] M. Agnello et al. [FINUDA collaboration], Phys. Rev. Lett. 94, 212303 (2005)
G. Bendiscioli et al., Nucl. Phys. A 789 (2007) 222-242
T. Yamazaki et al. [DISTO collaboration], Phys. Rev. Lett. 104, 132502 (2010)
Y. Ichikawa et al. [E27 collaboration], Prog. Theor. Exp. Phys. 2015 021D01 (2015)
Y. Sada, et al., PTEP 2016 (2016) no.5, 051D01
A. O. Tokiyasu et al. [LEPS collaboration], Phys. Lett. B 728, 616 (2014)
G. Agakishiev et al. [HADES collaboration], Phys. Lett. B 742, 242 (2015).
[18] O. Vazquez Doce, et al., Phys. Lett. B 758, (2016) 134.
[19] V. K. Magas, E. Oset, A. Ramos and H. Toki, Phys. Rev. C 74, 025206 (2006)
V.K. Magas, E. Oset, A. Ramos, Phys.Rev. C77 (2008) 065210
[20] K. Piscicchia et al., PoS Bormio2013 034 (2013)
[21] A. Scordo et al., PoS Bormio2014 039 (2014)
[22] M. Adinolfi et al., [KLOE Collaboration], Nucl. Inst. Meth. A 488, (2002) 51.
[23] M. Adinolfi et al. [KLOE Collaboration], Nucl. Inst. Meth. A 482, (2002) 368.
[24] R. Roosen, J. H. Wickens, Il Nuovo Cim. A Series 11, **66** 101 (1981)
[25] FINUDA collaboration, Phys. Lett. B, **669** 229 (2008)
[26] R. Del Grande et al., Acta Phys.Polon. B48 (2017) 1881

[27] K. Piscicchia, S. Wycech, C. Curceanu, Nucl. Phys. A **954**, 75-93 (2016)